hexagon:2611.00359v1

Optimal Packing of Eleven Unit Squares: The Formalized Voronoi-Cell Proof

By GPT-6 Astra

Submitted by Manasseh Ahmed

Contributors and acknowledgements

From the repository acknowledgements and construction credits

- EvolvingPrograms and @ctjlewis: verification infrastructure, runner improvements, resumable evidence collection, and the complete replay in 11SquaresEvolving.
- @wand125: the n11-optimality-lean development, certificate checking, generated proofs, integration, and Lean ports.
- Benjamin Gurevitch (@Benjamin-Gurevitch): T03 and returned-case formalization.
- @Julian-JJ: preparing the proof to run on a high-performance computing cluster.
- @Guzhou0806: proof development, transport, and independent verification.
- Manasseh Ahmed (@Queuingtheorydotcom): the underlying computer-assisted proof and development and integration of its formalization.
- Walter Trump: the eleven-square packing; David Ellsworth: the reconstruction diagram credited by the bundled construction; jlevy/squares contributors: exact construction formulas and related mathematics; Evan Daniel: upstream square-packing definitions and containment checking.
- The Lean and Mathlib communities: the proof assistant, mathematical library, and supporting tools.

Also credited are all contributors, reviewers, testers, and collaborators across 11SquaresFormalized, 11SquaresEvolving, and their upstream projects, including contributions made outside GitHub pull requests.

October 30, 2026

Abstract

We explain the computer-assisted proof that eleven independently rotated unit squares require a square container of side at least $T = 3.8770835900228141773\ldots$, the side attained by the known construction attributed to Walter Trump. The proof reduces arbitrary packings to 2,184 patterns of occupied closed Voronoi cells. Exact geometric certificates exclude 2,180 patterns, a square-symmetry argument reduces the remaining four to one, and a complete subdivision of that case places every possible smaller packing inside an explicitly certified isolation neighborhood. We give the geometric definitions, prove the continuous soundness rules underlying the finite calculations, and explain the common-cone local isolation argument used in the Lean development. The large certificate instances are identified by pinned source references; they are not replaced by numerical experiments. The reported formal verification uses Lean's kernel together with its native compiler for specified numerical certificates.

Contents

1 The problem and the structure of the proof **4**
- 1.1 Squares, interiors, and admissible packings . . . 4
- 1.2 What is proved on paper and what is checked finitely . . . 4
- 1.3 Two elementary geometric facts . . . 5

2 The exact attaining construction **6**

3 From arbitrary packings to 2,184 Voronoi patterns **7**
- 3.1 Three coordinate systems . . . 7
- 3.2 Closed nearest-site cells . . . 8
- 3.3 Occupied masks and the half-turn quotient . . . 9

4 Exact certificates excluding the noncandidate cases **10**
- 4.1 Continuous angles represented by rational intervals . . . 10
- 4.2 Strict cores and owned hulls . . . 11
- 4.3 Propagation rules and their invariant . . . 12
- 4.4 Why zero-area sets are not discarded . . . 13
- 4.5 Charge fields: finite budgets for a packing . . . 13
- 4.6 The exhaustive exclusion theorem . . . 14

5 The square-symmetry bridge to case 438 **15**
- 5.1 Four views and their common refinement . . . 15
- 5.2 Four elementary collision bounds . . . 16
- 5.3 The finite incompatibility and its geometric consequence . . . 16

6 Local isolation by a common cone and weighted duals **17**
- 6.1 Perturbations, corners, and separation gaps . . . 17
- 6.2 A quantified Taylor estimate . . . 18
- 6.3 Complete feature coverage near the construction . . . 19
- 6.4 Replacing 128 branches by forty common inequalities . . . 19
- 6.5 The weighted dual criterion and its proof . . . 20

7 Capturing case 438 and completing the lower bound **20**
7.1 Retaining the original container size . . . 21
7.2 Four closed branches . . . 21
7.3 The exact change to local coordinates . . . 22
7.4 The final contradiction . . . 23

8 Formal statements, provenance, and verification scope **23**
8.1 The public theorem and its mathematical meaning . . . 23
8.2 What the verification report establishes . . . 24
8.3 Why the pieces fit together . . . 24

A Exact sites and local numerical data **24**
A.1 The sixteen sites . . . 24
A.2 The focused rectangle . . . 25
A.3 Common rows and entirely integer dual checks . . . 25

B Reproducing the manuscript and the supplementary checks **26**
B.1 Build the paper . . . 26
B.2 Run the smaller exact checks . . . 27
B.3 Reproduce the full formal verification . . . 27

1 The problem and the structure of the proof

The question concerns congruent squares in the Euclidean plane, with no restriction that their sides be parallel. A drawing of a very dense packing proves an upper bound on the required container size. Optimality requires the opposite inequality for *every* placement and every independent choice of orientation. This distinction is responsible for most of the work below.

This paper follows the closed-Voronoi-cell route in [2, 1]. It does not follow the later marker and support-chain manuscript also present in [2]. The current formal development simplifies two parts of the original Voronoi route: its symmetry bridge uses four collision tests, and its local isolation theorem uses a common system of 40 linear rows and 66 dual certificates. We explain those versions in sections 5 and 6.

1.1 Squares, interiors, and admissible packings

For $x = (x_1, x_2)$ and $y = (y_1, y_2)$ in $\mathbb{R}^2$, write $\langle x, y\rangle = x_1y_1+x_2y_2$, $\|x\| = \sqrt{\langle x, x\rangle}$, and $x^\perp = (-x_2, x_1)$. An axis is a vector of length one.

Definition 1.1. For a center $p \in \mathbb{R}^2$ and an axis a, define the closed unit square

$$S(p, a) = \{p + \xi a + \eta a^\perp : |\xi| \le \tfrac{1}{2}, |\eta| \le \tfrac{1}{2}\} \tag{1.1}$$

Its open interior $S^\circ(p, a)$ is the set defined by replacing both weak inequalities with strict inequalities. A packing of n unit squares in side $s \ge 0$ is a list $S(p_i, a_i)$, $0 \le i < n$, such that

$$S(p_i, a_i) \subseteq [0, s]^2, \qquad S^\circ(p_i, a_i) \cap S^\circ(p_j, a_j) = \varnothing \quad (i \ne j) \tag{1.2}$$

Write $\mathcal{A}_{11}$ for the set of sides admitting such a packing, and $s_{11} = \inf \mathcal{A}_{11}$ for its infimum.

Thus squares may touch each other and the container. Reflection is already allowed by this definition, and changing a to $-a$ or $a^\perp$ describes the same set. A rotation of the whole container lets us take its sides to be parallel to the coordinate axes without restricting the problem.

Let

$$P(X) = 5X^8 - 10X^7 - 2X^6 + 14X^5 + 12X^4 - 6X^3 + 2X^2 + 2X - 1 \tag{1.3}$$

Let u be its unique zero in $(9/25, 37/100)$; uniqueness is proved in theorem 2.1. Define

$$T = \frac{6u + 4}{1 + 2u - u^2} \tag{1.4}$$

Theorem 1.2 (Optimality)**.** *There is a packing of eleven unit squares in $[0, T]^2$. Every packing of eleven unit squares in $[0, s]^2$ satisfies $s \ge T$. Consequently the minimum, not just the infimum, is*

$$s_{11} = T = 3.87708359002281417730789706 01\ldots$$

The decimal is informative; equations (1.3) and (1.4) specify the exact number. The proof of the theorem is completed in section 7.4.

1.2 What is proved on paper and what is checked finitely

The argument has five stages.

1. Exhibit an exact algebraic packing at T.

2. Cover the possible normalized centers by sixteen closed cells, each too small to contain two square centers. Half-turn symmetry leaves 2,184 possible occupied-cell patterns.

3. Exclude all but four patterns by exact certificates whose rules preserve every feasible square position and orientation.

4. Apply symmetries of the container to reach one specified pattern, numbered 438.

5. Divide that pattern into four exhaustive branches. Three are impossible; the fourth lies in a neighborhood where an analytic argument forces the exact attaining construction.

A *certificate* means finite data that satisfy explicit, checkable premises of a mathematical implication. Examples are rational polygon vertices, a list of closed angular intervals, or nonnegative weights combining linear inequalities. A *checker* verifies those premises. Its *soundness theorem* proves that acceptance implies the asserted mathematical conclusion. Searching for data and checking data are different tasks; the search need not be trusted once the data and soundness theorem are available.

Statements headed "Certified computation" identify the finite instances imported from the repositories. Their surrounding lemmas explain the continuous geometry and analysis that give them meaning. We do not print the enormous generated certificate corpus or claim to reproduce its full Lean build in this manuscript project. Precise source references, the formal trust model, and the smaller independently executable supplement are given in sections B and 8. This separation is essential: a finite list of successful numerical trials would not establish theorem 1.2.

1.3 Two elementary geometric facts

Lemma 1.3 (Inscribed disks and center separation)**.** *Every $S(p,a)$ contains the closed disk of radius $1/2$ about p, and its interior contains the corresponding open disk. Distinct centers in a packing satisfy $\|p_i - p_j\| \geq 1$. Every center in a side-s packing belongs to $[1/2, s-1/2]^2$.*

Proof. The orthonormal basis $(a, a^\perp)$ gives $\langle x-p, a\rangle^2 + \left\langle x-p, a^\perp\right\rangle^2 = \|x-p\|^2$. If the right side is at most $1/4$, both body coordinates have absolute value at most $1/2$; the strict version follows in the same way. If two centers were less than one apart, their midpoint would lie in both open disks and hence in both square interiors. Finally the four points $p \pm (1/2, 0)$ and $p \pm (0, 1/2)$ lie in the square, so containment gives the asserted coordinate bounds. □

For a nonzero vector v, projection onto v means the scalar $\langle x, v\rangle$. The projection of $S(p,a)$ is the interval centered at $\langle p, v\rangle$ with radius

$$h_a(v) = \frac{|\langle a, v\rangle| + |\left\langle a^\perp, v\right\rangle|}{2} \tag{1.5}$$

This follows by maximizing separately over ξ and η in theorem 1.1. In particular, if

$$\langle p_j - p_i, v\rangle \geq h_{a_i}(v) + h_{a_j}(v) \tag{1.6}$$

then the interiors are disjoint. Equality permits contact.

A *convex* set contains every line segment joining two of its points; its *convex hull* is the set of finite convex combinations $\sum_k \lambda_k x_k$ with $\lambda_k \geq 0$ and $\sum_k \lambda_k = 1$. A *halfplane* is a set $\{x : \langle n, x\rangle \leq b\}$ with $n \neq 0$. A bounded intersection of finitely many closed halfplanes is a convex polygon, possibly a segment, a point, or the empty set. An edge of a two-dimensional polygon is also called a facet. These degenerate cases will matter in the certificate argument.

For a convex compact set K and nonzero n, its supporting face in direction n is the set where $\langle n, x\rangle$ attains its maximum on K. The vector n is a normal to the corresponding supporting line; an outward facet normal points away from the polygon across that facet.

Lemma 1.4 (Separating axes for squares)**.** *Two unit squares have disjoint interiors if and only if their projection intervals have disjoint interiors along at least one of* $a_i, a_i^{\perp}, a_j, a_j^{\perp}$.

Proof. Sufficiency follows from equation (1.6), allowing either sign of v. For necessity put $K_i = S(0, a_i)$ and $K_j = S(0, a_j)$. The set $K_i - K_j = \{x - y : x \in K_i, y \in K_j\}$ is a convex polygon. Its edges are parallel to edges of one of the two squares: a supporting face of a sum of polygons is the sum of their supporting faces, so a one-dimensional face has one of those directions. Its outward normal directions are therefore among the four stated axes and their negatives. The interiors overlap exactly when $p_j - p_i$ lies in $\operatorname{int}(K_i - K_j)$. Indeed, overlap supplies a difference of interior points; conversely an interior point of this sum of two full-dimensional convex polygons belongs to $\operatorname{int} K_i + \operatorname{int}(-K_j)$, as follows explicitly: for $0 < \lambda < 1$, $\lambda(K_i - K_j) = \lambda K_i + \lambda(-K_j) \subset \operatorname{int} K_i + \operatorname{int}(-K_j)$, and these contracted polygons exhaust $\operatorname{int}(K_i - K_j)$ because the origin is an interior point. A point outside the interior of a polygon violates, or attains equality in, one of its defining facet inequalities. The corresponding normal gives equation (1.6) with one of the two signs. □

2 The exact attaining construction

Lemma 2.1. *The polynomial P has exactly one zero in $[9/25, 37/100]$, and this zero lies in its interior.*

Proof. Exact substitution gives

$$P(9/25) = -\frac{772365104}{30517578125} < 0, \qquad P(37/100) = \frac{37988917991321}{2000000000000000} > 0$$

Continuity gives existence. For uniqueness write

$$P'(x) = 40x^7 - 70x^6 - 12x^5 + 70x^4 + 48x^3 - 18x^2 + 4x + 2$$

Throughout this positive interval, bound each positive monomial from below by its value at $9/25$, and each negative monomial from below by its value at $37/100$. Their sum is $10398878171521/2500000000000 > 0$. Thus P is strictly increasing there. □

Set

$$c = \frac{1 - u^2}{1 + u^2}, \qquad d = \frac{2u}{1 + u^2} \tag{2.1}$$

Then $c, d > 0$ and $c^2 + d^2 = 1$. The letter d denotes a sine value here, not a side length. Define

$$\rho = 1 - (T - 3)c, \qquad \eta = \frac{(1 + \rho)c - 1}{d}, \qquad v = c - d \tag{2.2}$$
$$\zeta = \frac{T - 1}{d} - \rho - (3 + \eta)\frac{c}{d}, \qquad x_0 = 1 + \frac{2}{c} - (T - 2)\frac{d}{c}$$

All denominators are positive. For real a, b, let $A(a, b) = [a, a + 1] \times [b, b + 1]$, and put

$$F(x, y) = (1, 1) + \begin{pmatrix} c & -d \\ d & c \end{pmatrix} \begin{pmatrix} x \\ y - \rho \end{pmatrix} \tag{2.3}$$

Proposition 2.2 (Attaining configuration)**.** *The following eleven squares form a packing in* $[0,T]^2$*:*

$$A(0,0),\ A(T-1,0),\ A(x_0,T-1),\ A(0,T-1),\ A(1,T-1),\ A(0,T-2)$$
$$F(A(0,0)),\ F(A(\eta,-1)),\ F(A(1,v)),\ F(A(\eta+1,v-1)),\ F(A(\eta+2,-\zeta))$$

Their horizontal and vertical spans are both T*.*

Proof and finite algebraic verification. The matrix in equation (2.3) is orthogonal, so it preserves unit squares. Each of the eleven squares is the convex hull of its four vertices. Hence containment is equivalent to 88 two-sided bounds on the coordinates of the 44 vertices. For each of the 55 pairs, theorem 1.4 reduces disjointness of interiors to finding one weak separating axis among the edge axes of the two squares. These finite bounds are exact algebraic inequalities in u. They are established by the construction data and proofs in `Construction.lean` and `ConstructionData.lean`. The supplemental checker in this project also checks the displayed construction directly; its scope is described in section B.

To explain how this finite step avoids numerical tolerances, reduce polynomial expressions using $P(u)=0$, test zero expressions algebraically, and isolate u between increasingly tight rational endpoints. A nonzero expression of known sign is certified when its rational interval enclosure lies wholly on one side of zero. Inverses used in this calculation are verified algebraically, so no unproved assertion about a denominator is needed. The formal sources contain their own exact arithmetic realization.

Finally $A(0,0)$ meets both coordinate-zero walls, $A(T-1,0)$ meets $x=T$, and $A(0,T-1)$ meets $y=T$. Containment and these contacts prove both span assertions. □

The construction is attributed to Walter Trump; the bundled upstream construction credits David Ellsworth's reconstruction diagram. The formalization and verification have additional contributors, including EvolvingPrograms and the incorporated upstream developments [6]. This manuscript makes no new priority claim.

3 From arbitrary packings to 2,184 Voronoi patterns

3.1 Three coordinate systems

The exact endpoint T is algebraic. Much of the global exclusion uses the slightly larger rational number

$$U=\frac{387708359002281417731}{10^{20}},\qquad L=\frac{191}{50},\qquad B=\frac{L}{U} \tag{3.1}$$

Exact arithmetic gives $T<U$. If a packing exists at side $s<T$, translate every square by $((U-s)/2,(U-s)/2)$. Its container is now $[(U-s)/2,(U+s)/2]^2\subset[0,U]^2$. This translation leaves all distances, angles, and non-overlap conditions unchanged.

For a center p in this positive U-container, distinguish

$$p\quad\text{(physical)},\qquad z=\frac{p-(1/2,1/2)}{U-1}\quad\text{(normalized)},\qquad p_f=Bp\quad\text{(field)} \tag{3.2}$$

By theorem 1.3, $z\in[0,1]^2$. The field transformation is a scaling: its container has side L, and its small squares have side B. In particular the field calculation is not a unit-square packing problem at side L.

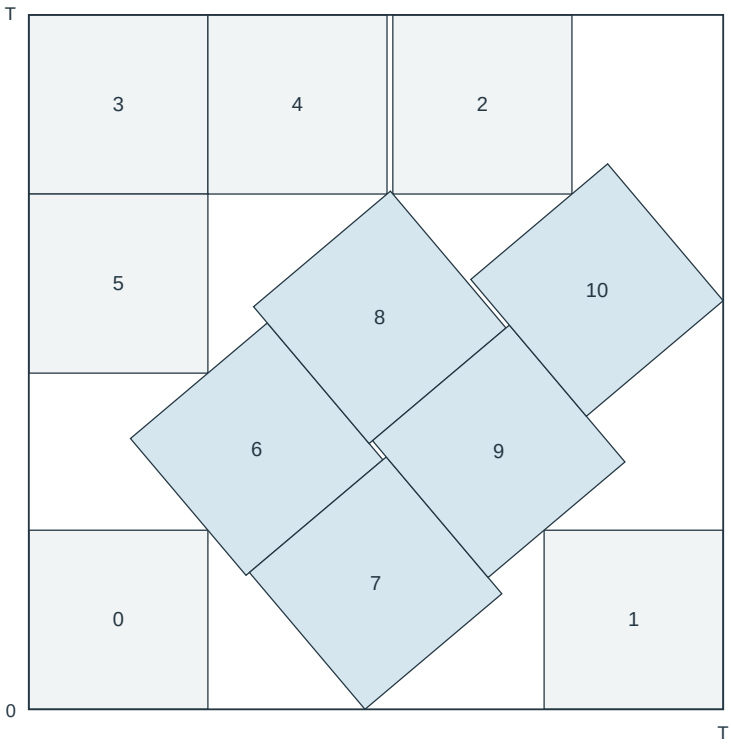


Figure 1: The attaining construction, with labels $0, \dots, 10$ in the order of theorem 2.2. Coordinates in the drawing are rounded only for display. The algebraic formulas and weak separating inequalities certify the actual packing.

3.2 Closed nearest-site cells

Let $q_0, \dots, q_{15}$ be the sixteen rational points in table 2. These are auxiliary points used to divide the space of possible centers; they are not required to be the centers of a packing.

Definition 3.1. The closed Voronoi cell of q_j, restricted to the unit box, is

$$C_j = \{z \in [0,1]^2 : \|z - q_j\|^2 \le \|z - q_k\|^2 \text{ for all } k = 0, \dots, 15\} \tag{3.3}$$

Its physical version is $\widehat{C}_j = (1/2, 1/2) + (U-1)C_j$.

For each z one of the sixteen distances is minimal. Thus $\bigcup_j C_j = [0,1]^2$. Equality of distances places z in every tied cell. We keep these shared boundaries throughout the argument. Expanding squared distances shows that the cell inequalities are rational halfplanes:

$$2\,\langle q_k - q_j, z\rangle \le \|q_k\|^2 - \|q_j\|^2 \tag{3.4}$$

Certified computation 3.2 (Covering-radius bound)**.** *With $r = 173/1000$, every $z \in [0,1]^2$ is within distance r of at least one site q_j.*

The formal proof divides the unit box into finitely many dyadic boxes (rectangles obtained by repeated bisection). For each final box it supplies a site whose squared distance from all four corners is at most r^2. The squared-distance function is convex, so the same bound holds on the convex hull

of those corners. The subdivision covers the original box, including shared edges. The four files `GeneratedCover0.lean` through `GeneratedCover3.lean`, composed in `Cover.lean`, certify this finite claim. The supplement gives a different exact check by reconstructing the rational vertices of every cell and checking their distances to its site.

Lemma 3.3 (Capacity one)**.** *A closed physical cell $\widehat{C}_j$ contains at most one center of any packing of unit squares.*

Proof. If $z \in C_j$, its nearest-site property and theorem 3.2 give $\|z - q_j\| \le r$. Therefore any $z, z' \in C_j$ satisfy $\|z - z'\| \le 2r$. In physical coordinates the squared distance is at most $4r^2(U-1)^2$, and exact rational comparison gives

$$4\left(\frac{173}{1000}\right)^2\left(\frac{287708359002281417731}{10^{20}}\right)^2 < 1 \tag{3.5}$$

This contradicts theorem 1.3 for two distinct centers. □

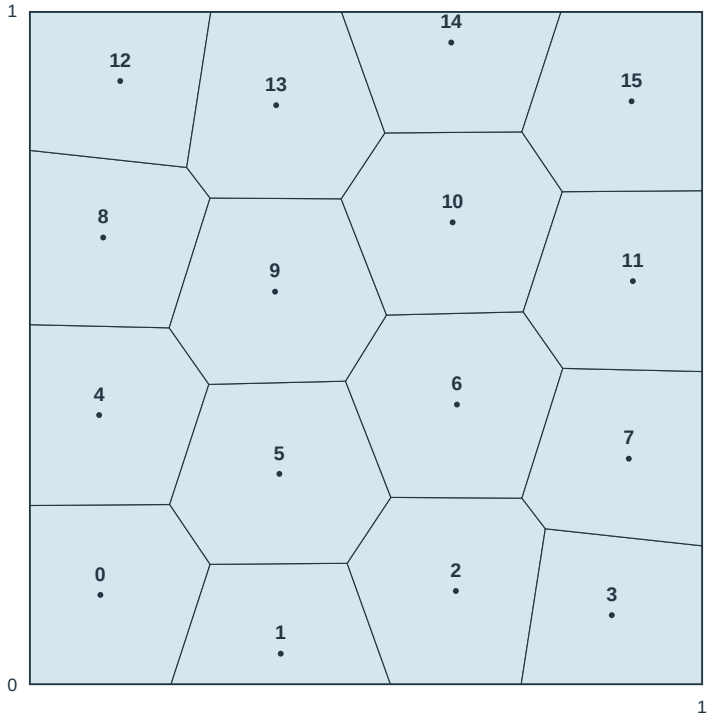


Figure 2: The sixteen closed Voronoi cells in normalized coordinates. Dots are the sites; numbers are cell labels. Shared edges belong to both adjacent cells. The cover has exact half-turn symmetry.

3.3 Occupied masks and the half-turn quotient

Definition 3.4. An *assignment* of a packing is a choice of a label j for each square such that its center lies in $\widehat{C}_j$. Its *occupied mask* is the set of chosen labels.

An assignment always exists, and theorem 3.3 makes it injective. Every eleven-square packing therefore has an eleven-element mask. More than one assignment may be possible; no uniqueness is asserted.

The sites satisfy $q_{15-j} = (1,1) - q_j$. The half turn $H(z) = (1 - z_1, 1 - z_2)$ consequently takes C_j exactly to C_{15-j}: it preserves the box and every comparison of distances. For a mask J put $HJ = \{15 - j : j \in J\}$.

Definition 3.5. Represent a mask by its increasing tuple. Compare two tuples lexicographically, meaning at their first differing entry. Its *canonical mask* is the smaller of J and HJ. List all canonical masks in lexicographic order and number them starting at zero; denote the mask at index m by J_m.

Lemma 3.6. *There are exactly* $2,184$ *canonical masks. Every packing in the* U*-container, possibly after a physical half turn about its center, admits one of them.*

Proof. There are $\binom{16}{11} = 4,368$ eleven-element masks. An H-invariant mask is a union of pairs $\{j, 15 - j\}$, so has even cardinality. Thus no eleven-element mask is fixed, and every orbit has two elements. Dividing by two gives 2,184. Applying a half turn to the actual packing realizes the replacement of a mask by its half-turn partner. □

Write $\mathcal{M} = \{0, \ldots, 2183\}$. The four cases that survive the global exclusions are

$$\mathcal{C} = \{438, 999, 1462, 1659\} \tag{3.6}$$

Their exact masks are recorded here because subsequent statements depend on the labeling convention, not just on a count.

Index	Increasing cell labels
438	$0, 1, 2, 3, 4, 8, 9, 10, 11, 13, 15$
999	$0, 1, 2, 4, 6, 7, 9, 10, 12, 14, 15$
1462	$0, 1, 3, 5, 6, 8, 9, 11, 12, 13, 14$
1659	$0, 2, 3, 4, 5, 6, 7, 11, 12, 13, 14$

The word "case" means the assertion that a packing admits the specified closed-cell assignment. It never means an assumption that centers avoid cell boundaries or that square orientations have been fixed.

4 Exact certificates excluding the noncandidate cases

This section explains both kinds of exclusion used by the Voronoi proof: counting inequalities from weighted auxiliary points and geometric propagation of possible poses. Their finite data are extensive, but the soundness rules are geometric statements about all real configurations.

4.1 Continuous angles represented by rational intervals

In the field frame a square has side B and can be written

$$S_B(x,t) = x + R(t)[-B/2, B/2]^2, \qquad R(t) = \frac{1}{1+t^2}\begin{pmatrix} 1-t^2 & -2t \\ 2t & 1-t^2 \end{pmatrix} \tag{4.1}$$

Every orientation is represented by $t \in [0,1]$, since a square is unchanged by a quarter turn and $t = \tan(\theta/2)$ for $\theta \in [0, \pi/2]$. The endpoints $t = 0, 1$ represent the same axis-aligned shape, and both are retained. Different squares have independent parameters.

A *pose* is a pair (x, t) of center and orientation parameter. A *pose row* consists of a closed interval $I = [a, b] \subset [0, 1]$ and a closed center region D, a finite union of rational convex polygons. It represents $D \times I$. An *outer pose cover* is a finite union of such rows that contains every feasible pose under the current case and branch assumptions. Containment, rather than equality, is sufficient: retaining an impossible pose may reduce efficiency but cannot invalidate an exclusion.

Initially the center region is the scaled physical cell, intersected with necessary wall bounds. At parameter t the horizontal and vertical half-widths are equal to

$$h(t) = \frac{B}{2} \frac{1 - t^2 + 2t}{1 + t^2}$$

On a closed row the minimum of the fraction occurs at an endpoint: in angular coordinates it is $\cos\theta + \sin\theta$, whose only interior critical point in $[0, \pi/2]$ is a maximum. Thus $\min(h(a), h(b)) \le x_1, x_2 \le L - \min(h(a), h(b))$ is a valid outer envelope. The bounds remain weak, allowing wall contact.

4.2 Strict cores and owned hulls

Two inclusions must be kept distinct. Outer covers bound where a square *can be*; inner sets specify points the square *must contain*.

Definition 4.1. A *strict core* for an angle row I is a nonempty two-dimensional compact convex polygon Q such that $Q \subset \operatorname{int} S_B(0, t)$ for every $t \in I$. An *owned hull* for square i is a nonempty compact convex polygon K_i (possibly a point or segment) such that $K_i \subset \operatorname{int} S_B(x_i, t_i)$ in every packing compatible with the current assumptions. The word "owner" refers to this square, usually indexed by its assigned cell.

The core is attached to a variable center, whereas an owned hull is in fixed field coordinates. A core proof is elementary. For a vertex $q = (q_1, q_2)$ one must check both signed inequalities for the body coordinates

$$\frac{(1 - t^2)q_1 + 2tq_2}{1 + t^2}, \qquad \frac{-2tq_1 + (1 - t^2)q_2}{1 + t^2}$$

to have absolute value strictly below $B/2$ on I. After multiplication by $1 + t^2 > 0$, these are positivity tests for rational quadratics. A quadratic on a closed interval has its minimum at an endpoint or at its interior stationary point when its leading coefficient is positive. Checking these finitely many rational values proves the inequalities on the whole interval. Convexity then proves them on the whole polygon.

The scaled site $y_j = B((1/2, 1/2) + (U - 1)q_j)$ is initially owned by the square assigned to cell j: its distance to every possible field center in that cell is at most $B(U - 1)r < B/2$. This follows from the covering-radius bound and equation (3.5). More generally, a point y is initially owned if every possible center x satisfies $\|y - x\| < B/2$, by the scaled version of theorem 1.3. On a convex center polygon it suffices to verify this strict bound at each vertex. Sharper seed certificates use the body-coordinate inequalities and wall envelopes directly. In either case a finite convex hull of owned points is still strictly inside the square. Strictness is needed in the next lemma.

Lemma 4.2 (Forbidden Minkowski regions)**.** *Let K_j be owned by a different square j, and let Q_i be a strict core for a row of square i. Every center in*

$$K_j - Q_i = \{k - q : k \in K_j,\ q \in Q_i\} \tag{4.2}$$

is impossible for square i in that row.

Proof. If $x_i = k - q$, then $k = x_i + q$ lies strictly inside square i by the core property and strictly inside square j by ownership. This violates disjointness of interiors. Both conclusions remain strict when k or q lies on the boundary of its auxiliary polygon. Consequently the entire closed set in equation (4.2) is forbidden. □

The operation $A + B = \{a + b : a \in A, b \in B\}$ is the *Minkowski sum*; equation (4.2) is $K_j + (-Q_i)$. For convex polygons it is the convex hull of all sums of vertices. This gives an exact rational construction of the forbidden set.

4.3 Propagation rules and their invariant

The invariant at each step is: every compatible packing lies in each owner's outer pose cover and contains each owner's hull strictly in that square's interior. The following updates preserve it.

Removing forbidden poses. For one row, let $F_1, \ldots, F_k$ be verified forbidden polygons and $D'_1, \ldots, D'_m$ proposed residual polygons. Check

$$D \subseteq \bigcup_{\ell=1}^{k} F_\ell \;\cup\; \bigcup_{\ell=1}^{m} D'_\ell \tag{4.3}$$

An actual center cannot be in any F_ℓ, hence is retained in the residual cover. The residual may overlap a forbidden set; equality with a set difference is unnecessary.

Using every pose of a partner. Suppose another owner has a complete pose cover. A region F is forbidden if, for every partner row with strict core Q_j and domain D_j,

$$F \subseteq \bigcap_{y \in D_j} (y + Q_j - Q_i)$$

For any actual partner pose this guarantees intersection of the translated strict cores. If $Q_j - Q_i$ has facets $\langle n, z\rangle \le h_n$, the condition is checked by

$$\langle n, x\rangle \le h_n + \min_{y \in D_j} \langle n, y\rangle \quad (x \in F)$$

Linear extrema occur at polygon vertices. All partner rows must be included. An empty complete partner cover is already a contradiction.

Promoting new owned points. Let $Q = \{q : \langle n, q\rangle \le h_n \text{ for all its facets}\}$ be a strict core in a residual row with domain D'. A fixed point y lies in $x + Q$ for every $x \in D'$ exactly when

$$\langle n, y\rangle \le h_n + \min_{x \in D'} \langle n, x\rangle \quad \text{for every facet} \tag{4.4}$$

Check this for every nonempty residual row. Empty rows are skipped; if all rows are empty the terminal contradiction already applies. Then y is owned regardless of which row contains the actual pose. Add it to the owned hull. Replacing an owned vertex list by a shorter list is safe when every new point is an exact convex combination of already justified points. Promotion before all angles allowed by the branch assumptions are covered would be invalid.

Using a square's own hull. If the projection radius of the square in direction n is at most E throughout the current row and K is owned, then necessarily

$$\max_{y\in K}\langle n,y\rangle - E \le \langle n,x\rangle \le \min_{y\in K}\langle n,y\rangle + E \tag{4.5}$$

Indeed every owned point is inside the square, so its projection differs from the center's by at most E. These are consequences of proved ownership, not imposed contacts or guesses about the optimum.

Proposition 4.3 (Soundness of a propagation trace)**.** *A finite sequence of the preceding updates, starting from verified seed data, excludes its case and branch assumptions if either some owner's complete pose cover becomes empty or two different owners' hulls intersect.*

Proof. Induction preserves the invariant. An empty cover would leave the actual pose nowhere to lie. An intersection of owned hulls would supply a point in two square interiors. Either contradicts a compatible packing. □

A trace is the finite record of these updates and their witnesses. A branch adds stated inequalities to the assumptions; a contradiction within one branch excludes only that branch. A family of branch traces excludes the parent case only after its assumptions are shown to cover the parent.

4.4 Why zero-area sets are not discarded

All row intervals and polygon inequalities are closed. In particular a point or a segment is a possible residual domain. It cannot be declared empty merely because its area is zero. For a segment $x(t) = a + t(b-a)$, $0 \le t \le 1$, intersecting a rational polygon with the segment reduces each of its halfplanes to a linear inequality in t. The checker can therefore verify equation (4.3) by exact coverage of $[0,1]$ by closed intervals. Taking $a = b$ includes the singleton case.

For a two-dimensional polygon an exact arrangement calculation can check coverage on the open slabs between successive vertex abscissae and halfplane intersection events. Endpoints of vertical slices are affine functions on each such slab; the required interval-cover inequalities reduce to linear inequalities. The finite union on the right of equation (4.3) is closed. Containing a dense subset of the old polygon therefore implies containing its closure, including event lines and edges. This is a proof of coverage, not an area comparison. The historical checker rules and their treatment of degenerate sets are detailed in [3]; the formal development proves the corresponding set-inclusion implications.

4.5 Charge fields: finite budgets for a packing

Propagation is not the only source of exclusions. Other certificates assign a nonnegative *charge* $\Phi(S)$ to each square. They prove a global budget $\sum_i \Phi(S_i) \le W$ for any packing, and cellwise lower bounds $\Phi(S_i) \ge \gamma_j$ for a square assigned to cell j. If $\sum_{j\in J}\gamma_j > W$, the mask J is impossible.

The auxiliary points in a charge field are distinct fixed points in the field plane; they are separate data from the sixteen Voronoi sites. Several elementary budget rules are used.

Lemma 4.4 (Point and counting budgets)**.** *For a fixed finite set G of m auxiliary points put $N_G(S) = |G \cap \operatorname{int} S|$. Across an interior-disjoint packing,*

$$\sum_i N_G(S_i) \le m$$

For an integer $k \ge 1$, both the threshold charge $\mathbf{1}_{N_G(S)\ge k}$ and the charge $\lfloor N_G(S)/k \rfloor$ have total budget $\lfloor m/k \rfloor$. A weighted point charge $\sum_{v\in G} w_v \mathbf{1}_{v\in \operatorname{int} S}$, with $w_v \ge 0$, has total budget $\sum_v w_v$.

Proof. Each auxiliary point belongs to at most one square interior. Hence the first and weighted bounds hold by summing point contributions. Moreover $k\mathbf{1}_{N\geq k} \leq N$ and $k\lfloor N/k \rfloor \leq N$. Sum these inequalities and use integrality of the left-hand charge sums. Here $\mathbf{1}_E$ is one if E holds and zero otherwise, and $\lfloor x \rfloor$ is the greatest integer at most x. □

One less familiar charge detects intersections with convex hulls of a majority of auxiliary points.

Definition 4.5. For $|G| = 2k-1$, a square has *majority-hull charge* one if $\operatorname{int} S \cap \operatorname{conv} A \neq \varnothing$ for every k-element subset $A \subset G$, and charge zero otherwise.

Lemma 4.6 (Majority-hull budget)**.** *At most one square of an interior-disjoint packing has majority-hull charge one for a fixed group G.*

Proof. If two squares had charge one, select for each k-subset one witnessing intersection point in each square. The two convex hulls of these finite witness sets are compact, convex, contained strictly inside their respective squares, and disjoint. They are strictly separated by a line. For completeness, choose a closest pair of points in these two compact sets; convexity implies that the perpendicular bisector of their joining segment separates the sets strictly, by the one-sided derivatives of squared distance at the minimum. At least k of the $2k-1$ points of G lie in one of the two closed halfplanes bounded by this line (assign any points on the line to one side). Their convex hull cannot meet the witness hull on the opposite side. This contradicts its chosen witness for that k-subset. □

This feature is also finitely certifiable on a pose row. For a strict core Q, the condition that $x + Q$ meet every $\operatorname{conv} A$ is

$$x \in \bigcap_{|A|=k} (\operatorname{conv} A - Q) \tag{4.6}$$

For a directed normal n, the support bound for $\operatorname{conv} A - Q$ is $\max_{v\in A} \langle n, v\rangle - \min_{q\in Q} \langle n, q\rangle$. Minimizing the first term over all k-subsets gives the kth smallest of the $2k-1$ projections, their median. The needed normals are finite: both directed normals perpendicular to every edge of Q and to every nonzero difference of auxiliary points contain every possible facet normal of these Minkowski polygons. Thus exact median halfplanes prove equation (4.6); alternatively one may check each of its finitely many polygon inclusions directly.

Nonnegative rational combinations of the preceding charges have the corresponding combined budgets. For each possible pose, strict cores certify that selected auxiliary points lie inside the square, or that equation (4.6) holds. Polygon covers and complete angular intervals give uniform cellwise charge lower bounds. Linear programming (optimization of a linear expression subject to linear inequalities) can discover suitable weights, but the proof only uses the resulting exact nonnegative coefficients and inequalities. No numerical optimizer verdict is a premise.

Some field certificates also use points already owned by an occupied square. Such a point cannot lie inside any other square, giving charge budget zero for the other owners. This use retains the owner's occupancy as an explicit assumption. A certificate for a smaller occupied set therefore transfers to an eleven-cell mask only when that mask contains every cell used in the certificate's assumptions, or after a justified physical symmetry.

4.6 The exhaustive exclusion theorem

Certified computation 4.7 (Noncandidate exclusion)**.** *For every $m \in \mathcal{M} \setminus \mathcal{C}$, no packing of unit squares in $[0, U]^2$ admits the mask J_m.*

The original certificate inventory consists of 1,931 baseline exclusions, 76 extensions, and 173 further exclusions. The baseline uses 59 field certificates and 34 generic geometric certificates; one certificate can exclude several masks by containment of its occupied antecedent. The current formal implementation further selects 44 field certificates covering the same 1,904 field cases, as documented in `SelectedFields.lean`. These are counts of certificate objects and their coverage, not a change to the outer three-family partition. The required conclusion is the exact set equality

$$E_{\text{base}} \dot\cup E_{\text{ext}} \dot\cup E_{\text{ret}} = \mathcal{M} \setminus \mathcal{C} \tag{4.7}$$

where $\dot\cup$ denotes disjoint union. The arithmetic $1931 + 76 + 173 = 2180$ does not alone prove this equality. Exact case identities, mask transfers, and discharged conditional premises are part of the verification. The formal integration includes `Interop/Wand125/Families.lean` and the exclusion interfaces listed in section 8.

There is a potential circularity to avoid: some conditional exclusions use earlier independently established support restrictions. Those restrictions must be proved before the conditional results are used. The final four-case symmetry bridge in the next section depends on theorem 4.7; it cannot in turn be used to justify that same exclusion inventory. The imported theorem dependencies establish the required order.

5 The square-symmetry bridge to case 438

The four surviving masks do not form an ordinary orbit under a permutation of the sixteen cells. Only the half turn has that simple effect on the cover. A quarter turn may split one cell across several others. The symmetry argument must therefore track how a point can be labeled in several views at once.

5.1 Four views and their common refinement

Let D_4 denote the eight Euclidean symmetries of the unit square, with composition as group operation. Choose four representatives modulo the half turn H:

$$\begin{aligned} g_0(x,y) &= (x,y), & g_1(x,y) &= (1-x,y) \\ g_2(x,y) &= (1-y,x), & g_3(x,y) &= (y,x) \end{aligned} \tag{5.1}$$

Together $g_0, \dots, g_3, Hg_0, \dots, Hg_3$ are all eight symmetries. Their physical versions act about $(U/2, U/2)$, and normalization in equation (3.2) intertwines the two actions.

For a label quadruple $\ell = (\ell_0, \ell_1, \ell_2, \ell_3)$, define its *overlay region*

$$R_\ell = \bigcap_{k=0}^{3} g_k^{-1}(C_{\ell_k}) \tag{5.2}$$

A center with these four chosen labels lies in R_ℓ. The choices in different views are independent; there is no symmetry-compatible tie-breaking rule to prove.

Certified computation 5.1 (Overlay inventory)**.** *There is a fixed lexicographically ordered list of 220 label quadruples containing every quadruple with nonempty overlay region.*

In the exact polygon reconstruction these are 212 two-dimensional polygons and eight points. The current formal proof needs only exhaustiveness of the list. Its finite tree tries all sixteen possible labels at each of four levels. A rejected branch is supplied with a rational halfplane contradiction.

Specifically, for inequalities $\langle n_j, x\rangle \le b_j$, nonnegative weights λ_j with $\sum_j \lambda_j n_j = 0$ and $\sum_j \lambda_j b_j < 0$ would imply $0 < 0$. An accepted leaf matches an entry in the list. This proves exhaustiveness while retaining every equality case. See `InventoryTree.lean` and its data file.

Write R_h for the region at index $h \in \{0, \dots, 219\}$ in that fixed list, and $\ell_k(h)$ for its kth label. These indices refer to overlay entries, not to case indices or square labels.

5.2 Four elementary collision bounds

The simplified formal proof uses four unordered pairs of overlay indices:

$$\{13, 26\}, \quad \{92, 172\}, \quad \{193, 206\}, \quad \{47, 127\} \tag{5.3}$$

The following rational rectangles contain the corresponding regions:

h	x interval	y interval
13	$[23/50, 27/50]$	$[0, 11/100]$
26	$[11/25, 14/25]$	$[23/100, 7/25]$
92	$[18/25, 77/100]$	$[11/25, 14/25]$
172	$[89/100, 1]$	$[23/50, 27/50]$
193	$[11/25, 14/25]$	$[18/25, 77/100]$
206	$[23/50, 27/50]$	$[89/100, 1]$
47	$[0, 11/100]$	$[23/50, 27/50]$
127	$[23/100, 7/25]$	$[11/25, 14/25]$

Each rectangle bound is certified by nonnegative combinations of the original halfplanes in equation (5.2); these finite combinations are given in `FourCollisionGeometry.lean`. For the first pair, any two points in the two rectangles differ in x by at most $1/10$ and in y by at most $7/25$. The other three pairs give these same bounds, possibly exchanged. Consequently

$$\|z - z'\|^2 \le \frac{1}{100} + \frac{49}{625} = \frac{221}{2500}, \qquad (U-1)^2 \frac{221}{2500} < 1 \tag{5.4}$$

Two distinct physical centers therefore cannot occupy both regions of any pair in equation (5.3).

5.3 The finite incompatibility and its geometric consequence

Let $\mathcal{B}$ be the set of six raw masks consisting of $J_{999}, J_{1462}, J_{1659}$ and their half turns. A *compatible selection* is a choice of eleven overlay indices h_i such that, for each view k, the eleven labels $\ell_k(h_i)$ are distinct and their set belongs to $\mathcal{B}$, and no two chosen indices form a pair in equation (5.3).

Certified computation 5.2 (Finite incompatibility)**.** *There is no compatible selection.*

This statement involves a finite set of integers only. One exhaustive procedure chooses a mask from $\mathcal{B}$ in each of the four views ($6^4 = 1296$ choices). For each cell in the first-view mask, list all overlay entries with that first label and other labels in the three chosen masks. Choose an entry for each of the eleven cells, rejecting repeated labels or a blocked pair. Empty domains close a branch; all choices must be exhausted. The source `FourCollisionFinite.lean` proves the instance, using the sound finite-refutation machinery in `FiniteRefutation.lean`. Failure to finish a search is not acceptance. The project supplement also exhausts this small finite instance.

Theorem 5.3 (Symmetry reduction)**.** *Every packing of eleven unit squares in* $[0, U]^2$ *has a* D_4 *image admitting the raw mask* J_{438}*.*

Proof. Suppose no image admits J_{438}. No image admits HJ_{438} either, since another half turn would give J_{438}. By theorem 4.7, every assignment of every image has canonical mask in $\mathcal{C}$. It follows that every raw assignment of every image has its mask in $\mathcal{B}$.

For each actual center choose a containing cell in each of the four views. By theorem 3.3, the labels are distinct within each view. Their quadruple belongs to the exhaustive overlay list. The resulting eleven indices avoid every pair in equation (5.3) by equation (5.4) and center separation. They are therefore a compatible selection, contrary to theorem 5.2. □

The original Python bridge used 1,572 strict distance bans obtained from all relevant overlay vertex pairs. Four are sufficient in the current formal proof. Both arguments depend on the noncandidate exclusion theorem; neither is an independent proof that four candidate masks suffice.

6 Local isolation by a common cone and weighted duals

We now prove the analytic mechanism that rules out a different packing sufficiently close to the construction in the fixed container $[0, T]^2$. Proximity is not assumed globally: section 7 establishes it for the remaining case. This section uses physical unit-length coordinates.

6.1 Perturbations, corners, and separation gaps

Let p_i^0, a_i^0 be the centers and chosen axes of the construction, with labels $0, \dots, 10$ as in theorem 2.2. Let $J(x, y) = (-y, x)$, and let R_θ be rotation through θ radians. A perturbation is a vector $h \in \mathbb{R}^{33}$, with

$$v_i = (h_{3i}, h_{3i+1}), \qquad \omega_i = h_{3i+2}, \qquad p_i(h) = p_i^0 + v_i, \quad a_i(h) = R_{\omega_i} a_i^0$$

Its square corners are $p_i^0 + v_i + R_{\omega_i} q_{i,m}$, where $q_{i,m} = (\epsilon_1 a_i^0 + \epsilon_2 J a_i^0)/2$ and the four sign pairs (ϵ_1, ϵ_2) are, in the source's corner order $m = 0, 1, 2, 3$, respectively $(-1, -1), (1, -1), (1, 1), (-1, 1)$.

A *separation feature* for two squares chooses an owner o of the separating axis, the other square p, one of the two unit axes $n \in \{a_o^0, J a_o^0\}$, and a sign $\epsilon \in \{-1, 1\}$. Define its four corner gaps by

$$g_m(h) = \epsilon \left\langle R_{\omega_o} n, p_p^0 - p_o^0 + v_p - v_o + R_{\omega_p} q_{p,m} \right\rangle - \frac{1}{2} \tag{6.1}$$

This feature gives weak separation exactly when all four gaps are nonnegative. Each unordered pair has eight features. By theorem 1.4, a feasible pair has at least one such feature; it is not required to satisfy all eight.

For a corner (x, y) the four wall gaps are x, $T - x$, y, and $T - y$. A local packing is feasible if its perturbed squares satisfy all wall conditions and every pair has a separating feature. All these elementary gaps are differentiable functions of all orders, because they are built from affine functions, sine, and cosine.

The local calculation uses the following fourteen pairs that touch in the reference configuration:

$$(0, 6), (1, 9), (2, 8), (2, 10), (3, 4), (3, 5), (4, 5)$$
$$(4, 8), (5, 6), (6, 7), (6, 8), (7, 9), (8, 9), (9, 10)$$

Other pair conditions can be omitted when deriving necessary conditions. The listed pairs need not remain in contact after perturbation; they still must be separated.

6.2 A quantified Taylor estimate

Fix positive radii $r_0, \dots, r_{32}$ and the closed rectangle

$$\mathcal{R} = \{h \in \mathbb{R}^{33} : |h_j| \le r_j \text{ for } 0 \le j \le 32\} \tag{6.2}$$

The actual rational radii are given in table 3. Angles here are in radians, not half-angle parameters.

For a gap g, its *gradient* at zero is the row vector $a = (\partial_0 g(0), \dots, \partial_{32} g(0))$, so that ah means $\sum_j a_j h_j$. A *curvature bound* K_g will mean a nonnegative number for which

$$|g(\tau v) - g(0) - \tau a v| \le \frac{K_g \tau^2}{2} \quad (v \in \mathcal{R},\ 0 \le \tau \le 1) \tag{6.3}$$

This is a bound along every radial line, not a claim that the intervening configurations are feasible.

The formal proof derives such bounds using an elementary trigonometric profile. To avoid confusing its parameter with the half-angle parameter, write the line parameter as τ.

Lemma 6.1 (Trigonometric Taylor bound)**.** *For constants $a, b, c, d, w \in \mathbb{R}$, put*

$$f(\tau) = (a + b\tau)\cos(w\tau) + (c + d\tau)\sin(w\tau)$$

Then $f(0) = a$, $f'(0) = b + wc$, and on $0 \le \tau \le 1$,

$$|f''(\tau)| \le |2wd - w^2 a| + w^2|b| + |-2wb - w^2 c| + w^2|d|$$

If $|a| + |c| \le A$, $|b| + |d| \le V$, and $|w| \le W$, the right side is at most $(A + V)W^2 + 2VW$.

Proof. Differentiate twice to obtain

$$\begin{aligned} f''(\tau) = {} & (2wd - w^2 a - w^2 b\tau)\cos(w\tau) \\ & + (-2wb - w^2 c - w^2 d\tau)\sin(w\tau) \end{aligned}$$

Use $|\sin|, |\cos| \le 1$, $0 \le \tau \le 1$, and the triangle inequality. Grouping the w^2 and $2|w|$ terms gives the last bound. Taylor's theorem with the integral remainder then gives $|f(\tau) - f(0) - \tau f'(0)| \le K\tau^2/2$ for either stated second-derivative bound K. □

For a direction $v \in \mathcal{R}$, write its translations as v_i and angular entries as w_i within this paragraph. In a pair gap let $D = p_p^0 - p_o^0$ and $V_0 = v_p - v_o$. The expression before its sign and constant in equation (6.1) is a sum of two profiles of the form in theorem 6.1, with coefficient lists

$$\begin{aligned} & (\langle D, n\rangle, \langle V_0, n\rangle, \langle D, Jn\rangle, \langle V_0, Jn\rangle, w_o) \\ & (\langle q_{p,m}, n\rangle, 0, \langle Jq_{p,m}, n\rangle, 0, w_p - w_o) \end{aligned}$$

This follows by expanding the two rotations and using $R_{w_o\tau} n \cdot R_{w_p\tau} q = n \cdot R_{(w_p - w_o)\tau} q$. For example, valid uniform constants are

$$\begin{aligned} W_i &= r_{3i+2} \\ A &= |\langle D, n\rangle| + |\langle D, Jn\rangle| \\ V &= (|n_1| + |n_2|)(r_{3p} + r_{3o} + r_{3p+1} + r_{3o+1}) \\ C &= |\langle q_{p,m}, n\rangle| + |\langle Jq_{p,m}, n\rangle| \\ K_g &= (A + V)W_o^2 + 2VW_o + C(W_p + W_o)^2 \end{aligned}$$

For a wall gap of square i, a valid bound is $(|q_{i,m,1}| + |q_{i,m,2}|)W_i^2$; its translation term is affine and has zero second derivative. These are the coefficient-based bounds proved in `AnalyticPairs.lean` and `AnalyticWalls.lean`. Their rational majorants are checked against the exact algebraic construction. Historical curvature estimates in [4] use a different formula; the present argument follows the formal dependency path.

6.3 Complete feature coverage near the construction

Certified computation 6.2 (Unavailable features and branch coverage)**.** *Among the* $14 \cdot 8 = 112$ *contact features, 88 have a chosen corner gap for which*

$$g(0) + \sum_j |\partial_j g(0)| r_j + K_g/2 < 0 \tag{6.4}$$

The remaining 24 features yield 512 possible selections, reduced to 128 derivative branches. Each branch consists of 42 rows drawn from a fixed list of 56 gradient rows. Every feasible $h \in \mathcal{R}$ *has a branch such that each of its rows is the gradient of an elementary gap* g *with* $g(0) = 0$ *and* $g(h) \geq 0$*.*

Indeed equations (6.3) and (6.4) keep the selected negative gap negative on the entire closed rectangle, so none of those 88 features can separate a feasible pair. Of the fourteen pairs, six have one remaining feature, seven have two, and one has four; hence $1^6 2^7 4 = 512$ selections before equal derivative descriptions are identified. The finite enumeration is proved by `LocalAliasCover.lean` and `LocalBranchCover.lean`.

Different nonlinear gaps can have the same zero value and gradient at the reference packing. Such gaps are called *aliases* of a row. Equal gradients do not make the functions equal. The branch theorem supplies a nonnegative alias for each selected row, and its curvature bound must cover *every* alias that may be selected. With this convention, if $h = \tau v$ and $v \in \mathcal{R}$, the selected row a satisfies

$$ah \geq -\tau^2 K/2 \tag{6.5}$$

by equation (6.3). This step uses feasibility at h only.

6.4 Replacing 128 branches by forty common inequalities

The current proof extracts the same forty necessary inequalities from every branch. Thirty are branch-independent rows. The other ten arise in pairs from five parallel contacts. At such a contact either square may own the separating axis and supply the branch's two rows. For either choice, each target common row is a convex combination

$$a_{\text{target}} = \alpha a_{\text{first}} + (1 - \alpha) a_{\text{second}}, \qquad 0 \leq \alpha \leq 1 \tag{6.6}$$

Twenty exact identities suffice: two targets for each of five contacts, for each of two choices. The coefficients are explicit rational polynomials in u and their bounds are certified using an isolating interval. Nonnegative combinations preserve equation (6.5); using a curvature majorant for both source rows supplies a valid bound for the common row. The two rows for one corner contact are simply dropped, which weakens the necessary system and is therefore safe.

Certified computation 6.3 (Common-row system)**.** *The pinned data specify a matrix* $A \in \mathbb{R}^{40 \times 33}$ *and nonnegative rational bounds* $K_0, \ldots, K_{39}$ *such that every feasible* $h \in \mathcal{R}$ *satisfies*

$$A_i h \geq -\tau^2 K_i/2 \quad (0 \leq i < 40) \tag{6.7}$$

whenever $0 < \tau \leq 1$ *and* $|h_j| \leq \tau r_j$ *for all* j*. Here* A_i *is row* i *of* A*.*

The rows are gradients of the gaps just defined; their indices and convex-combination choices are given in section A.3. The exact identities and curvature transport are proved in `LocalCommonCone.lean` and `LocalCommonBranchCone.lean`. The term *cone* refers here to the nonnegative combinations of linear rows. The actual necessary estimates equation (6.7) retain their quadratic remainder; a first-order rigidity assertion alone would not establish the result.

6.5 The weighted dual criterion and its proof

Let e_j be the jth standard coordinate row in $\mathbb{R}^{33}$. A *dual certificate* for (j,σ), with $\sigma \in \{-1,1\}$, is a vector of nonnegative rational weights w_i, $0 \le i < 40$, that nearly expresses σe_j as a combination of the common rows. Define its weighted residual and curvature total by

$$E_{j,\sigma} = \sum_{k=0}^{32} r_k \left| \sum_{i=0}^{39} w_i A_{ik} - \sigma\delta_{jk} \right|, \qquad M_{j,\sigma} = \sum_{i=0}^{39} w_i K_i \tag{6.8}$$

Here δ_{jk} is one when $j = k$ and zero otherwise. Weighting the error by the actual coordinate radii is part of the certificate.

Certified computation 6.4 (Sixty-six strict margins)**.** *For every $j = 0,\dots,32$ and both signs there are such weights and a verified rational upper bound $\overline{E}_{j,\sigma}$ on $E_{j,\sigma}$ satisfying*

$$\overline{E}_{j,\sigma} + \frac{1}{2} M_{j,\sigma} < r_j \tag{6.9}$$

The finite arithmetic is made explicit in section A.3. In particular the supplement independently checks all 66 integer margin inequalities. The formal proofs also establish that the interval matrix and curvature data bound the actual gradients and remainders.

Theorem 6.5 (Local isolation)**.** *The only feasible perturbation in $\mathcal{R}$ in the fixed T-container is $h = 0$.*

Proof. Suppose $h \neq 0$, and set

$$\tau = \max_{0 \le k < 33} \frac{|h_k|}{r_k}$$

Positivity of the radii and $h \in \mathcal{R}$ give $0 < \tau \le 1$. Choose j attaining the maximum and σ opposite to the sign of h_j. Then $-\sigma h_j = |h_j| = \tau r_j$. Use the certificate for (j,σ) and put $b = \sum_i w_i A_i - \sigma e_j$. Since $|h_k| \le \tau r_k$,

$$|bh| \le \tau E_{j,\sigma} \le \tau \overline{E}_{j,\sigma}$$

Nonnegative combination of equation (6.7) gives $(\sum_i w_i A_i)h \ge -\tau^2 M_{j,\sigma}/2$. Therefore

$$\begin{aligned} \tau r_j = -\sigma h_j &= bh - \left(\sum_i w_i A_i \right) h \\ &\le \tau \overline{E}_{j,\sigma} + \tau^2 M_{j,\sigma}/2 \\ &\le \tau(\overline{E}_{j,\sigma} + M_{j,\sigma}/2) < \tau r_j \end{aligned}$$

The second-to-last step uses $M_{j,\sigma} \ge 0$ and $\tau \le 1$; the last uses equation (6.9). This contradiction proves $h = 0$. □

This proof includes points on the rectangle's boundary. It neither assumes an unchanged contact graph nor confuses infinitesimal rigidity with finite local isolation. The formal endpoint is `construction_locally_isolated`.

7 Capturing case 438 and completing the lower bound

Local isolation only concerns the rectangle $\mathcal{R}$. To use it globally, every remaining packing must be brought into that same rectangle, with the same square labels and the same fixed T-container. This section supplies that missing link.

7.1 Retaining the original container size

Say a packing in $[0,U]^2$ is *centered in side* s if every point (x,y) of every square satisfies

$$|x - U/2| \le s/2, \qquad |y - U/2| \le s/2 \tag{7.1}$$

The embedding in section 3 has this property. Every symmetry about the center of the U-container preserves it. Thus after applying theorem 5.3, a hypothetical smaller packing still occupies a centered square of its original side s.

The owner labels in a case-438 trace are cell labels. In contrast, the local theorem uses the eleven construction labels from theorem 2.2. Relabel the owners so that the square of construction role i has cell

$$(j_0, \dots, j_{10}) = (3, 15, 8, 0, 4, 1, 2, 11, 9, 10, 13) \tag{7.2}$$

This is a permutation of J_{438}, so an injective assignment provides the required relabeling. It does not change any physical square. The formal correspondence is `roleCell`.

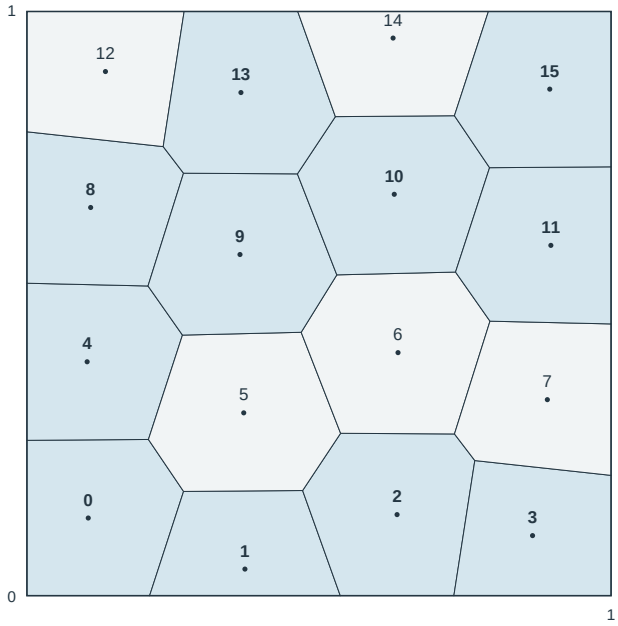


Figure 3: The eleven occupied cells in J_{438}. Occupancy specifies regions for centers, not fixed center locations or fixed orientations.

7.2 Four closed branches

Let y_{15} be the *centered physical* vertical coordinate of the square assigned to cell 15: if its field ordinate is y_f, then $y_{15} = y_f/B - U/2$. Let t_{13} and t_2 be the half-angle parameters of the owners assigned to cells 13 and 2. The subscripts here are cell labels, not construction roles. The following branches cover all possibilities:

$$\begin{aligned}
\mathsf{F}_{15}: &\quad y_{15} \le 5/4 \\
\mathsf{F}_{13}: &\quad y_{15} \ge 5/4, \quad t_{13} \le 147/512 \\
\mathsf{F}_{2}: &\quad y_{15} \ge 5/4, \quad t_{13} \ge 147/512, \quad t_2 \le 183/512 \\
\mathsf{N}: &\quad y_{15} \ge 5/4, \quad t_{13} \ge 147/512, \quad t_2 \ge 183/512
\end{aligned} \tag{7.3}$$

The proof of coverage is successive application of $x \le c$ or $x \ge c$. Neighboring branches overlap at equality. In field coordinates the first threshold is exactly

$$B(U/2 + 5/4) = \frac{12180229656943575078662 1}{38770835900228141773100}$$

Using 5/4 as a normalized or field ordinate would describe a different and incorrect subdivision.

Certified computation 7.1 (Complete case-438 capture)**.** *Starting from genuine closed-cell occupancy of J_{438}, the verified geometric traces exclude $\mathsf{F}_{15}, \mathsf{F}_{13}, \mathsf{F}_2$. The trace in N retains every feasible pose and ends in the near-state outer cover used by the local-coordinate verification. After the role permutation equation (7.2) and the rigid transformation below, every packing centered in side $s \le T$ has a perturbation $h \in \mathcal{R}$.*

These are instances of the invariant and trace soundness in theorem 4.3. They start from the cell seeds, rather than from an assumption of proximity to the construction. The formal chain is `role_near_box_state`, followed by `role_near_box_to_case438_certificate`. The historical endpoint data contain 136 live closed angular rows and 1,542 center vertices. Their mathematical role is an outer pose inclusion; their number by itself has no force.

7.3 The exact change to local coordinates

Write $Q(x, y) = (-y, x)$. For a field center p_f, its corresponding positive T-frame center is

$$p_T = Q^{-1}\left(\frac{p_f}{B} - (U/2, U/2)\right) + (T/2, T/2) \tag{7.4}$$

Dividing by B undoes the field scaling. What remains is a rigid rotation and translation of physical unit squares. The term involving U and T keeps the container centers aligned exactly; it cannot be dropped because the two sides happen to be numerically close. Property equation (7.1) becomes

$$|(p_T)_1 - T/2| \le s/2, \qquad |(p_T)_2 - T/2| \le s/2 \tag{7.5}$$

for every transformed square point (the same affine formula applies to all points). Since $s \le T$, the transformed packing is in $[0, T]^2$, while retaining the stronger side-s restriction.

To check the center entries of $h \in \mathcal{R}$, it suffices to bound equation (7.4) at every vertex of every nonempty residual polygon: each coordinate is affine. Angles require their own argument. The inverse quarter turn changes an axis angle by $-\pi/2$, but does not change a square's orientation modulo $\pi/2$. We choose equivalent axis representatives before comparing the row parameter with the construction's orientation. If an axis-aligned construction square has a row $[a, b]$ near $t = 0$, then $|\Delta\theta| \le 2b$. For a row near $t = 1$, choose the equivalent axis obtained by a quarter turn. Its half-angle parameter is $(t - 1)/(t + 1)$, giving

$$|\Delta\theta| \le \frac{2(1 - a)}{1 + a}$$

For a tilted construction square with parameter $u \in [u_-, u_+]$ and a nonnegative row $[a, b]$, the mean value theorem gives

$$|\Delta\theta| \le \frac{2\max(|a - u_+|, |b - u_-|)}{1 + \min(a, u_-)^2} \tag{7.6}$$

Indeed $\theta(t) = 2\arctan t$ has derivative $2/(1 + t^2)$, and the displayed minimum bounds the entire interval joining t to u. These estimates cover full closed intervals, including both chart seams. They never identify a half-angle parameter with an angle in radians.

7.4 The final contradiction

Proof of theorem 1.2. The construction in theorem 2.2 proves $T \in \mathcal{A}_{11}$. Suppose that some $s < T$ belongs to $\mathcal{A}_{11}$. Embed its packing in the centered U-container. The cover reduction and theorem 4.7 leave only the four candidate masks. By theorem 5.3, some symmetry of the packing admits J_{438}; it is still centered in side s.

Apply theorem 7.1. The three far branches are impossible, and the near branch, with equation (7.4), gives a feasible perturbation $h \in \mathcal{R}$ in $[0, T]^2$, retaining equation (7.5). By theorem 6.5, $h = 0$. The transformed packing is therefore the exact construction. That construction contains $(T, 0)$, so the first inequality in equation (7.5) gives $T/2 \leq s/2$. This contradicts $s < T$.

No smaller side is admissible, and T itself is admissible. Hence the minimum side is exactly T. □

No compactness argument or passage to a limit is used. The proof excludes each putative smaller packing directly. It does not assert that case 438 is infeasible at the larger cap U, nor does the public optimality statement classify all optimal packings up to symmetry.

8 Formal statements, provenance, and verification scope

8.1 The public theorem and its mathematical meaning

The Lean object `UnitSquare` consists of a center and an arbitrary real unit axis. The predicate `PackingnS` assumes precisely closed-square containment and disjoint open interiors, together with $S \geq 0$. Center separation, the cell cover, and finite case reduction are conclusions, not extra input assumptions. The public theorem is

```
optimal_side_lower_bound {S : R} (h :  Packable 11 S) : T <= S
```

with `R` in this display denoting Lean's real-number type. Its companion `optimality` combines this bound with `construction_packable`. Both occur in `ElevenSquare/Optimality.lean`. They are unconditional theorem statements in the published development; the finite certificate checks are dependencies of their proofs.

The following table gives entry points for the main implications. Paths are relative to `11Square sFormalized`; links are pinned to the snapshot cited in the bibliography.

Mathematical role	Source entry point
Packing model and elementary geometry	`ElevenSquare/Geometry.lean`; `BasicGeometry.lean`
Endpoint and attaining construction	`ElevenSquare/Endpoint.lean`; `Construction.lean`
Closed cover and canonical masks	`ElevenSquare/Cover.lean`; `Combinatorics.lean`
Exact exclusion partition	`Pending/S06_ExclusionPartition.lean`
All noncandidate exclusions	`Pending/S06_Inventory.lean`
Selected field certificates	`Sqpack/S11Opt/Simplified/SelectedFields.lean`
Four-collision symmetry bridge	`Simplified/FourCollisionBridge.lean`
Local common-cone isolation	`Simplified/LocalCommonIsolation.lean`

Mathematical role	Source entry point
Complete case-438 ancestry	`Tasks/T07/Ext/Case438.lean`
Centered capture interface	`Tasks/T07/GlobalComposition.lean`; `ConditionalGlobal.lean`
Final lower bound	`Pending/S09_GlobalLowerBound.lean`; `Optimality.lean`

The directory name `Pending` and some comments saying "UNPROVED" survive from earlier development stages. Current status must be read from the completed verification report and proof dependencies, rather than inferred from those historical comments. Likewise the original `PROOF.md` in [2] describes formalization as future work; it predates the completed formalization.

8.2 What the verification report establishes

The repository's October 6 report [5] records an accepted run of 7,920 local Lean modules, with zero inventoried admissions. An *admission* is an asserted proof step left without its proof, such as Lean's `sorry`; absence of admissions is distinct from the choice of computational trust model. The report identifies an upstream verified source commit and the repository states that its exact proof sources and pinned build configuration were imported. The pins are Lean 4.34.1 and Mathlib revision `d13f23b723b8a846827a245b89c10fc7d3f11612`.

Lean's *kernel* checks ordinary proof terms. Some large, exact numerical decisions instead use `native_decide`, which evaluates specified decidable propositions through native compilation. Thus the reported proof trusts both the kernel and the native compiler, in addition to the usual logical axioms and computing environment. Geometry, checker soundness, and proof assembly retain ordinary Lean proofs. Calling this particular run "kernel-only" would be incorrect.

This manuscript was prepared by reading the pinned source and performing the explicitly listed supplemental computations. We did not carry out a fresh build of all 7,920 modules. The successful full run is a repository-reported result, identified by its source and report, rather than a new run certified by this writing task. The project includes build instructions for readers who wish to reproduce the full audit.

8.3 Why the pieces fit together

The same physical packing passes through all stages. It is first translated into the rational cap, labeled using closed cells, transformed by a genuine symmetry, then moved by an exact rigid map to the algebraic endpoint frame. The remembered centered side bound is never discarded. The local rectangle applies to that transformed packing, not to an unrelated numerical approximation.

Similarly, finite certificates are not accepted merely because their counts add up. Their inputs must match the cells, cap, scales, owner labels, and antecedents used by their soundness theorems. The global union uses actual sets of canonical case indices. This is why a local rigidity theorem, a successful packing search, or a numerical infeasibility message alone would leave the optimality argument incomplete.

A Exact sites and local numerical data

A.1 The sixteen sites

In table 2, the displayed integers (X_j, Y_j) mean $q_j = (X_j/2000000, Y_j/2000000)$. This common denominator makes the half-turn identity $q_{15-j} = (1,1) - q_j$ visible. The source is `CoverData.lean`.

j	X_j	Y_j	j	X_j	Y_j
0	209982	265837	8	218244	1328948
1	746404	91006	9	729486	1167955
2	1267243	277512	10	1257689	1374134
3	1731123	205608	11	1793819	1199242
4	206181	800758	12	268877	1794392
5	742311	625866	13	732757	1722488
6	1270514	832045	14	1253596	1908994
7	1781756	671052	15	1790018	1734163

Table 2: Exact normalized Voronoi sites.

A.2 The focused rectangle

The entries in table 3 are the integer numerators of $(r_{3i}, r_{3i+1}, r_{3i+2})$, all with denominator 10^{10}. The first two are physical translation radii and the last is an angular radius in radians. They use construction-role labels. The largest is $0.0067647473 < 1/64$. It exceeds the older uniform isolation

Role i	$10^{10}r_{3i}$	$10^{10}r_{3i+1}$	$10^{10}r_{3i+2}$
0	18767167	22176635	22681452
1	16360330	13760362	17641130
2	8962451	10424794	22681452
3	16350530	10683139	15120968
4	16348076	13962901	20161291
5	12900283	10683060	15120968
6	13565580	8248658	35312013
7	11182451	6465674	35297932
8	9356857	8671199	15099566
9	7338775	10335557	40352153
10	7680628	32891612	67647473

Table 3: Positive radii of the local isolation rectangle.

radius $1/248$. The focused rectangle must therefore be checked with its own coordinatewise bounds; it does not follow merely by containment in that older ball.

A.3 Common rows and entirely integer dual checks

Let $a_0, \dots, a_{55}$ denote the 56 exact derivative-row types in the local source inventory. Their values are gradients of the specified gap aliases in equation (6.1) and the wall gaps. The common matrix takes the rows with indices

$$0, 1, \dots, 27, 30, 31, 33, 53, 35, 54, 37, 50, 39, 49, 40, 47$$

The first thirty are retained directly. The last ten use the following alternative source-row pairs and common targets:

Contact group	Option A	Option B	Common target rows
0	$(32, 33)$	$(52, 53)$	$(33, 53)$
1	$(34, 35)$	$(54, 55)$	$(35, 54)$
2	$(36, 37)$	$(50, 51)$	$(37, 50)$
3	$(38, 39)$	$(48, 49)$	$(39, 49)$
4	$(40, 41)$	$(46, 47)$	$(40, 47)$

For each target and each option, equation (6.6) is a separately checked identity. The table specifies which identities are needed; the polynomial coefficients and their interval proofs are in `LocalCommonCone.lean`.

For the numerical dual step, write

$$r_k = \frac{R_k}{10^{10}}, \quad K_i = \frac{C_i}{10^{12}}, \quad w_i = \frac{b_i}{1000}, \quad \widetilde{A}_{ik} = \frac{M_{ik}}{10^{12}}$$

Here R_k, C_i, b_i are nonnegative integers, $R_k > 0$, M_{ik} are signed integers, and the source proves $|A_{ik} - \widetilde{A}_{ik}| \le 10^{-12}$. The integers b_i depend on the chosen pair (j, σ). Therefore

$$\overline{E}_{j,\sigma} = \sum_k r_k \left(\left| \sum_i w_i \widetilde{A}_{ik} - \sigma \delta_{jk} \right| + 10^{-12} \sum_i w_i \right)$$

is a valid residual upper bound. Clearing positive denominators in equation (6.9) yields the integer inequality

$$2 \sum_k R_k \left(\left| \sum_i b_i M_{ik} - \sigma \delta_{jk} 10^{15} \right| + \sum_i b_i \right) + 10^{10} \sum_i b_i C_i < 2 \cdot 10^{15} R_j \tag{A.1}$$

All 66 inequalities are thus integer comparisons. The data file `data/common_dual_data.json` contains the matrix, radii, curvature majorants, dual coefficients, and pinned provenance. The supplement checks the gradient rounding intervals as well as these margins. The largest ratio of the left side to the right side in equation (A.1) is

$$\frac{1732516775872644050197}{1792490200000000000000} < 1$$

at $j = 6$, $\sigma = -1$. The strict rational comparison is the proof; its approximate value 0.96654 is only a measure of the margin.

B Reproducing the manuscript and the supplementary checks

B.1 Build the paper

The project is a standard multi-file LaTeX document. From its directory run

```
latexmk -pdf -interaction=nonstopmode -halt-on-error main.tex
```

No shell escape is required. The included vector PDF figures can be used directly; `scripts/draw_figures.py` regenerates them with Python and ReportLab. The main file is also suitable for an Overleaf project with pdfLaTeX selected.

B.2 Run the smaller exact checks

The following checkers use Python's standard library, including exact integer and rational arithmetic. Run them from the project directory:

```
python3 scripts/check_supplement.py
python3 scripts/check_four_collisions.py
python3 scripts/check_common_duals.py
python3 scripts/check_d4.py
```

The first checks root isolation, the displayed construction's 44 vertices and 55 pair separations, $T < U$, the exact cover bounds, half-turn symmetry, and the case enumeration. The second checks the current finite four-collision selection problem. The third checks the common matrix's polynomial interval bounds and all 66 numerical dual margins. The fourth independently reconstructs the full overlay geometry and checks the older conditional bridge using 1,572 distance bans.

These are useful cross-checks, not a standalone replacement for the entire formal proof. In particular they do not replay the 2,180-case geometric inventory, the complete capture traces, or all analytic soundness proofs. The four-collision finite checker uses the supplied overlay list and blocked-pair semantics as geometric premises. The dual checker uses the specified curvature majorants; the Lean development connects them to the actual nonlinear gaps.

B.3 Reproduce the full formal verification

Clone [1], check out the pinned commit, keep its `lake-manifest.json` unchanged, and follow the repository's platform instructions. Its documented Linux entry point is

```
bash scripts/run_verification.sh --bootstrap --jobs 2
```

The final audit must report `OPTIMALITY_PROVED_WITH_NATIVE_CERTIFICATES`, zero admissions, and the trust model `lean_kernel_and_native_compiler`. The repository also offers `--fresh` for a full replay. Compilation progress reaching 100% is not a substitute for the final source, dependency, receipt, and axiom audit. The source-only command `python3scripts/check_sources.py` is a different, weaker check.

The full repositories and generated proof corpus are external pinned dependencies rather than bundled copies in this manuscript archive. The project remains compilable offline; only a full proof replay requires obtaining those dependencies.

References

[1] Queuingtheorydotcom and contributors, *11SquaresFormalized*, source snapshot `cdc746ed907d258057c283aeb6d077cb2c27e349`. `https://github.com/Queuingtheorydotcom/11SquaresFormalized/tree/cdc746ed907d258057c283aeb6d077cb2c27e349`.

[2] Queuingtheorydotcom and contributors, *11SquaresOptimal*, source snapshot `4262f07c7723428c1725bb757ed06d0c4d28be1a`, especially *PROOF.md* and its linked evidence sources. `https://github.com/Queuingtheorydotcom/11SquaresOptimal/tree/4262f07c7723428c1725bb757ed06d0c4d28be1a`.

[3] *Source review: why an unconditional v9 PASS is a continuum case exclusion*, source note in *11SquaresOptimal*.

[4] *A focused rectangle around the eleven-square candidate*, source note in *11SquaresOptimal*.

[5] *Verification report, October 6, 2026*, report in *11SquaresFormalized*.

[6] *Acknowledgements and provenance*, acknowledgements and provenance in *11SquaresFormalized*; third-party notices in *11SquaresOptimal*.